Matrix Product States for Gauge Field Theories

Boye Buyens,[1] Jutho Haegeman,[1] Karel Van Acoleyen,[1] Henri Verschelde,[1] and Frank Verstraete[1,2]
[1]Department of Physics and Astronomy, Ghent University, Krijgslaan 281, S9, 9000 Gent, Belgium
[2]Vienna Center for Quantum Science and Technology, Faculty of Physics, University of Vienna, Boltzmanngasse 5, 1090 Vienna, Austria

(Received 28 February 2014; revised manuscript received 27 June 2014; published 25 August 2014)

The matrix product state formalism is used to simulate Hamiltonian lattice gauge theories. To this end, we define matrix product state manifolds which are manifestly gauge invariant. As an application, we study $(1+1)$-dimensional one flavor quantum electrodynamics, also known as the massive Schwinger model, and are able to determine very accurately the ground-state properties and elementary one-particle excitations in the continuum limit. In particular, a novel particle excitation in the form of a heavy vector boson is uncovered, compatible with the strong coupling expansion in the continuum. We also study full quantum nonequilibrium dynamics by simulating the real-time evolution of the system induced by a quench in the form of a uniform background electric field.

DOI: 10.1103/PhysRevLett.113.091601 PACS numbers: 11.15.−q, 02.70.−c, 05.10.Cc, 11.15.Tk

Gauge theories hold a most prominent place in physics. They appear as effective low-energy descriptions at different instances in condensed matter physics and nuclear physics. But first and foremost they lie at the root of our understanding of the four fundamental interactions that are each mediated by the gauge fields corresponding to a particular gauge symmetry. At the perturbative quantum level, this picture translates to the Feynman diagrammatic approach that has produced physical predictions with unlevelled precision, most famously in QED. However, the perturbative approach miserably fails once the interactions become strong. This problem is most pressing for QCD, where all low-energy features like quark confinement, chiral symmetry breaking, and mass generation are essentially nonperturbative.

Lattice QCD, which is based on Monte Carlo sampling of Wilson's Euclidean lattice version of gauge theories, has historically been by far the most successful method in tackling this strongly coupled regime. Using up a sizable fraction of the global supercomputer time, state-of-the-art calculations have now reached impressive accuracy, for instance, in the *ab initio* determination of the light hadron masses [1]. But in spite of its clear superiority, the lattice Monte Carlo sampling also suffers from a few drawbacks. There is the infamous sign problem that prevents application to systems with large fermionic densities. In addition, the use of Euclidean time, as opposed to real time, presents a serious barrier for the understanding of dynamical nonequilibrium phenomena. Over the past few years there has been a growing experimental and theoretical interest in precisely these elusive regimes, e.g., in the study of heavy ion collisions or early time cosmology.

In this Letter we study the application of tensor network states (TNS) as a possible complementary approach to the numerical simulation of gauge theories. This is highly relevant as this Hamiltonian method is free from the sign problem and allows for real-time dynamics. As a first application, we focus on the massive Schwinger model. For this model the TNS approach has been studied before by Byrnes *et al.* [2] and Bañuls *et al.* [3]. By integrating out the gauge field (which one can only do for $d = 1 + 1$), the model was reduced to an ordinary spin model, yet with a nonlocal Hamiltonian. Our approach is conceptually different, as we keep the gauge field degrees of freedom, which enables us to take the thermodynamic limit, with the relevant global symmetries exact. TNS have been considered also for the discrete $Z2$ gauge theory, for $d = 1 + 1$ by Sugihara [4], and for $d = 2 + 1$ by Tagliacozzo and Vidal [5].

Over the past decade the TNS framework has emerged as a powerful tool for the study of local quantum many body systems, exploring the fact that physical states (i.e., ground states and their low-energy excitations) occupy only a tiny corner of the full Hilbert space [6]. This is exemplified by the relatively small amount of quantum entanglement that these states possess. TNS are then trial quantum states that precisely capture this feature, allowing for relatively low cost numerical variational calculations. In one spatial dimension, they also go by the name of matrix product states (MPS), underlying the well-known density matrix renormalization group algorithm (DMRG) [7]. At present, MPS/DMRG is the state-of-the-art method in the numerical study of both static and dynamical properties of $d = 1 + 1$ strongly correlated condensed matter systems. And also in higher dimensions the TNS framework [8], although less developed, is considered to be a promising candidate for the numerical simulation of strongly interacting quantum many body systems.

The essential new ingredient with respect to the usual MPS applications on quantum many body systems is that for the Hamiltonian formulation of gauge theories, within

the full Hilbert space only the subspace of gauge-invariant states is actually physical. Although, due to Elitzur's theorem [9] gauge invariance will not be broken on the full Hilbert space, there will be typically many more low-energy excitations in the full space than in the constrained physical subspace. It is therefore crucial to restrict the variational MPS manifold to this physical subspace. Notice that the very same issue poses itself in the context of the simulation of gauge theories with ultracold atoms. See Ref. [10] for a recent proposal to implement gauge invariance in that case.

The massive Schwinger model is QED in $1+1$ dimensions, with one flavor of fermionic particles with mass m, interacting through a $U(1)$ gauge field with coupling g (which has mass dimension 1 for $d=1+1$). This model shares some interesting features with QCD, most notably the fermions are confined into zero charge bound states. Furthermore, in the continuum it can be studied by a strong coupling expansion [11,12], which makes it a perfect benchmark model. We will apply our gauge-invariant MPS construction on the Hamiltonian lattice formulation of the model, focusing on the strongly coupled regime $g/m \gtrsim 1$ and extrapolating our results to the continuum. We determine the ground state and stable bound states. In addition, we show how our formalism indeed allows for the study of real-time phenomena and simulate the full quantum dynamics induced by a background electric field.

The Schwinger Hamiltonian.—To write down a lattice Hamiltonian for the Schwinger model, one starts from the Lagrangian density in the continuum,

$$\mathcal{L} = \bar{\psi}[\gamma^{\mu}(i\partial_{\mu} + gA_{\mu}) - m]\psi - \frac{1}{4}F_{\mu\nu}F^{\mu\nu}. \tag{1}$$

One can then perform a Hamiltonian quantization in the timelike axial gauge ($A_0 = 0$), which can be turned in a lattice system by the Kogut-Susskind spatial discretization [13] with the two-component fermions sited on a staggered lattice. These fermionic degrees of freedom can then finally be converted to spin-1/2 degrees of freedom by a Jordan-Wigner transformation, leading to the gauged spin Hamiltonian (see Ref. [2] for more details),

$$H = \frac{g}{2\sqrt{x}}\left(\sum_{n\in\mathbb{Z}} L(n)^2 + \frac{\mu}{2}\sum_{n\in\mathbb{Z}}(-1)^n[\sigma_z(n) + (-1)^n] + x\sum_{n\in\mathbb{Z}}[\sigma^+(n)e^{i\theta(n)}\sigma^-(n+1) + \text{H.c.}]\right). \tag{2}$$

Here we have introduced the parameters $x \equiv 1/(g^2a^2)$ and $\mu \equiv 2\sqrt{x}m/g$, with a the lattice spacing.

The spins live on the sites of the lattice, with $\sigma_z(n)|s_n\rangle = s_n|s_n\rangle (s_n = \pm 1)$ and $\sigma^{\pm} = 1/2(\sigma_x \pm i\sigma_y)$ the spin ladder operators. Notice the different second (mass) term in the Hamiltonian for even and odd sites. This can be traced back to the staggered formulation, with the even sites being reserved for the "positrons" and the odd sites for the "electrons." For the even positron sites, $s_{2n} = +1$ can be viewed as an occupied state, while $s_{2n} = -1$ corresponds to an empty state, and vice versa for the odd electron sites. The gauge fields $\theta(n) = agA_1(na/2)$ live on the links between the sites. Their conjugate momenta $L(n)$, with $[\theta(n), L(n')] = i\delta_{n,n'}$, correspond to the electric field $gL(n) = E(na/2)$. Since $\theta(n)$ is an angular variable, $L(n)$ will have integer charge eigenvalues $p_n \in \mathbb{Z}$. The local Hilbert space, spanned by the corresponding eigenkets $|p_n\rangle$ is therefore infinite, but in practice we will do a truncation and consider $|p_n| \leq p_{\max}$ in a numerical scheme. For our calculations, we take $p_{\max} = 3$.

The Hamiltonian (2) is invariant under T^2, a translation over two sites, and the corresponding eigenvalues read $T^2 = e^{2ika}$, where k is the physical momentum of the state. Another symmetry that will be useful is CT, obtained by a translation over one site, followed by a charge conjugation, $C|s_n, p_n\rangle = |-s_n, -p_n\rangle$. Since $C^2 = 1$, we will have $CT = \pm e^{ika}$. The states with positive sign then correspond to the scalar sector, while the negative sign corresponds to the vector sector.

In addition, the Hamiltonian is invariant under the residual time-independent local gauge transformations, generated by

$$G_n = L(n) - L(n-1) - \frac{1}{2}[\sigma_z(n) + (-1)^n]. \tag{3}$$

It is this gauge invariance that sets the Hamiltonian quantization of gauge theories apart from the Hamiltonian quantization of ordinary systems. For gauge theories only the subspace of gauge-invariant states will be physical: $G_n|\Psi\rangle_{\text{phys}} = 0$ for every n. This is called the Gauss law constraint, as $G_n = 0$ is indeed the discretized version of $\partial_x E = \rho$. We will now show how one can tailor the MPS formalism towards a constrained variational method on this physical gauge-invariant subspace.

Gauge-invariant MPS.—A general, not necessarily gauge-invariant MPS for the lattice spin-gauge system (2), has the form

$$\sum_{s_n, p_n} \text{Tr}[B_1^{s_1} C_1^{p_1} B_2^{s_2} C_2^{p_2} \ldots C_{2N}^{p_{2N}}]|s_1, p_1, s_2, p_2 \ldots, p_{2N}\rangle, \tag{4}$$

where for now we consider a finite lattice of $2N$ sites. Here, each $B_n^{s_n}$ (and $C_n^{p_n}$) is a complex $D \times D$ matrix with components $[B_n^{s_n}]_{\alpha\beta}$ that constitute the variational parameters of the trial state. The indices $\alpha, \beta = 1, \ldots, D$ are referred to as virtual indices, and D is called the bond dimension.

Gauss's law [see Ref. (3)] prescribes how to update the electric field $L(n)$ at the right link of a site n, either staying with the value $L(n-1)$ at the left in case there is no charge at the site or adding (subtracting) one unit in case there is a positive (negative) charge at the site. This can be conveyed

by the matrix multiplications in a MPS by giving the virtual indices a multiple index structure $\alpha \to (q, \alpha_q)$, where q labels the charge, and taking the matrices of the form

$$[B_n^{s_n}]_{(q,\alpha_q),(r,\beta_r)} = [b_{n,q}^{s_n}]_{\alpha_q,\beta_r}\delta_{q+[s_n+(-1)^n]/2,r},$$
$$[C_n^{p_n}]_{(q,\alpha_q),(r,\beta_r)} = [c_n^{p_n}]_{\alpha_q,\beta_r}\delta_{q,p_n}\delta_{r,p_n}. \quad (5)$$

One can readily verify that a MPS (4) with matrices of this form indeed obeys the Gauss law constraint at every site. Conversely, we show in S1 of the Supplemental Material [14] that every gauge-invariant state $|\Psi\rangle$, obeying $G_n|\Psi\rangle = 0$ for every n, has a MPS representation of the form (5).

Ground state and excitations.—To obtain a ground-state approximation in the thermodynamic limit ($N \to \infty$), it will be useful to block a site and link into one site with the local Hilbert space spanned by the states $|q_{2n-1}\rangle = |s_{2n-1}, p_{2n-1}\rangle$ and $|q_{2n}\rangle = |s_{2n}, p_{2n}\rangle$. Anticipating $CT = 1$, the gauge-invariant ground state ansatz then takes a form similar to a uniform MPS (uMPS) [15],

$$|\Psi(A)\rangle = \sum_{q_n} v_L^\dagger \left(\prod_{n\in\mathbb{Z}} A^{q_n}\right) v_R |\boldsymbol{q}^c\rangle, \quad (6)$$

where $|\boldsymbol{q}^c\rangle = |\{(-1)^n q_n\}_{n\in\mathbb{Z}}\rangle$, v_L, $v_R \in \mathbb{C}^D$, and $A^q \in \mathbb{C}^{D\times D}$, as follows from (5),

$$[A^{s,p}]_{(q,\alpha_q);(r,\beta_r)} = [a^{s,p}]_{\alpha_q,\beta_r}\delta_{p,q+(s+1)/2}\delta_{r,-p}. \quad (7)$$

We refer to S2 of the Supplemental Material [14] for the details and implementation of the time-dependent variational principle (TDVP) [16] to obtain an approximation for the ground state. The variational freedom of the gauge-invariant state $|\Psi(A)\rangle$ lies within the matrices $a^{s,p} \in \mathbb{C}^{D_q\times D_r}$ and the total bond dimension of the uMPS equals $D = \sum_{q\in\mathbb{Z}} D_q$. It will be important to choose the distribution of D_q wisely, according to the relative weight of the different charge sectors. As illustrated in Fig. 1(a), this is done by looking at the Schmidt coefficients for an arbitrary cut and demanding that the smallest coefficients of each sector coincide more or less. The resulting distribution of D_q is peaked around $q = 0$ and justifies our $p_{\max} = 3$ truncation that corresponds to $D_q = 0$ for $|q| > 3$ (see also S3 of the Supplemental Material [14]).

Once we have a good approximation for the ground state, we can use the method of Refs. [17,18] to obtain the one-particle excited states. The excitations are labeled by their (physical) momentum $k \in [-\pi/2a, \pi/2a[$ and their CT quantum number $\gamma = \pm 1$. For a given ground-state approximation, we then take the following ansatz state $|\Phi_{k,\gamma}(B, A)\rangle$ for the one-particle excitations:

$$\sum_{m\in\mathbb{Z}} e^{ikma}\gamma^m \sum_{q_n} v_L^\dagger \left(\prod_{n<m} A^{q_n}\right) B^{q_m} \left(\prod_{n>m} A^{q_n}\right) v_R |\boldsymbol{q}^c\rangle, \quad (8)$$

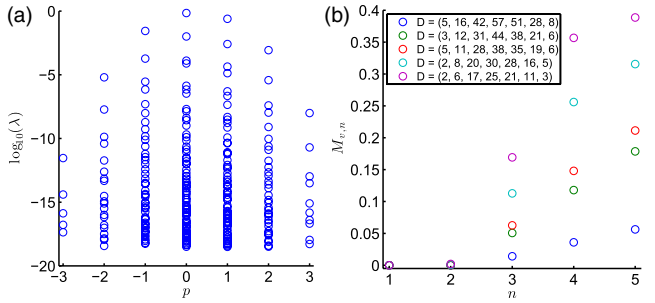

FIG. 1 (color online). Results for $m/g = 0.25$, $x = 100$. (a) Distribution of the (base-10) logarithm of the Schmidt coefficients λ in every charge sector for $D = (5, 20, 48, 70, 62, 34, 10)$. (b) Difference for the estimated energies of the excited states for various bond dimension with respect to these with $D = (5, 20, 48, 70, 62, 34, 10)$ for the vector sector $\gamma = -1$. Only the first two excitations are stable under variation over D.

with B^q again of the gauge invariant form (7) with general matrices $b^{s,p}$. These are determined variationally by minimizing their energy in the ansatz subspace, which leads to a generalized eigenvalue problem (see S2 of the Supplemental Material [14] for more details). For a given momentum and CT quantum number, we typically find different local minima of which only one or two are stable under variation of the bond dimension D [see fig. 1(b)]. It is these stable states that we can interpret as approximations to actual physical one-particle excitations.

In Table 1 we display our results for the continuum extrapolations $a \to 0$ ($x \to \infty$) of the ground-state energy density and the mass of the different one-particle excitations (we refer to S3 of the Supplemental Material [14] for more details). For $g/m \neq 0$, we find three excited states, one scalar and two vectors, with the hierarchy of masses $M_{v,1} < M_{s,1} < M_{v,2}$ matching that of the strong coupling result [11,12]. This is the first time that the second vector excitation has been found numerically. For the energy density and the two lowest mass excitations, our results are consistent with the previous most precise simulations [2,3], with a similar or sometimes better accuracy. As shown in the Supplemental Material, we were also able to reconstruct the Einstein dispersion relation for small momenta $ka \ll 1$.

TABLE I. Energy density and masses of the one-particle excitations (in units $g = 1$) for different m/g. The last column displays the result for the heavy vector boson, compatible with the prediction of Coleman and Adam [11,12].

m/g	ω_0	$M_{v,1}$	$M_{s,1}$	$M_{v,2}$
0	−0.318 320(4)	0.564 18(2)		
0.125	−0.318 319(4)	0.789 491(8)	1.472(4)	2.10(2)
0.25	−0.318 316(3)	1.019 17(2)	1.7282(4)	2.339(3)
0.5	−0.318 305(2)	1.487 473(7)	2.2004(1)	2.778(2)
0.75	−0.318 285(9)	1.963 47(3)	2.658 943(6)	3.2043(2)
1	−0.318 26(2)	2.444 41(1)	3.1182(1)	3.640(4)

Real-time evolution.—One of the main advantages of the TNS framework is that it allows for the full quantum simulation of real-time phenomena. Specifically, we have investigated the nonequilibrium dynamics induced by applying a uniform electric field E on the ground state $|\Psi_0\rangle$ at time $t = 0$. Physically, the process corresponds to the so-called Schwinger particle creation mechanism [19], but now for a confining theory. This process has been studied extensively in the past, either with some effective classical kinetic description [20,21] or in the semiclassical limit for the gauge fields [21–23] and recently also with the AdS/CFT correspondence [24]. Here we focus on the systematics of our method and present some first results, allowing us to validate our formalism against the predicted scaling from linear response theory and energy conservation. A more detailed analysis will be presented elsewhere [25].

In our setup the application of a uniform electric field is simulated by applying a uniform quench, replacing $L(n)$ with $L(n) + \alpha$ in the Hamiltonian (2), where $E = g\alpha$. As before, we define our ansatz by blocking a site and a link into one site. But since the background field now breaks CT invariance, we can anticipate translation symmetry $T^2 = 1$ over only two sites. Our ansatz thus takes the form

$$|\Psi(A_1, A_2)\rangle = \sum_{q_n} v_L^\dagger \left(\prod_{n\in\mathbb{Z}} A_1^{q_{2n-1}} A_2^{q_{2n}} \right) v_R |\{(q_{2n-1}, q_{2n})\}\rangle, \tag{9}$$

where $q_n = (s_n, p_n)$. From Eq. (5) it follows that gauge invariance is imposed if we set $[A_n^{s,p}]_{(q,\alpha_q);(r,\beta_r)} = [a_n^{s,p}]_{\alpha_q,\beta_r} \delta_{p,q+(s+(-1)^n)/2} \delta_{r,p}$.

To perfom the real-time evolution, we have implemented the infinite time-evolving block decimation algorithm (iTEBD) [26] using a fourth-order Trotter expansion [27] with time step $dt = 0.01/g$. We refer to S4 of the Supplemental Material [14] for the details. At every step iTEBD truncates the Hilbert space by discarding the Schmidt coefficients lower than some fixed threshold ϵ^2. For gauge invariant MPS this in turn determines the required bond dimensions D_p for every charge sector that will evolve in time. For instance, for the value $\epsilon_0 = 2 \times 10^{-6}$ that we used for the simulations in Figs. 2(b)–2(d), and for $\alpha = 0.3$, the maximal bond dimension goes from $D_0 = 18$ at $t = 0$ to $D_0 = 173$ at $t = 25$. It is this growth of the required bond dimensions, which can be traced back to the growth of entanglement, that makes the computations more costly at later times. As the simulation should be exact as $\epsilon \to 0$, the convergence in ϵ can be used to control the truncation error for a certain observable. We illustrate this in Fig. 2(a) for the electric field expectation value. Also notice that the convergence rate decreases in time. Keeping the truncation error small for larger time intervals will therefore require smaller values of the tolerance ϵ.

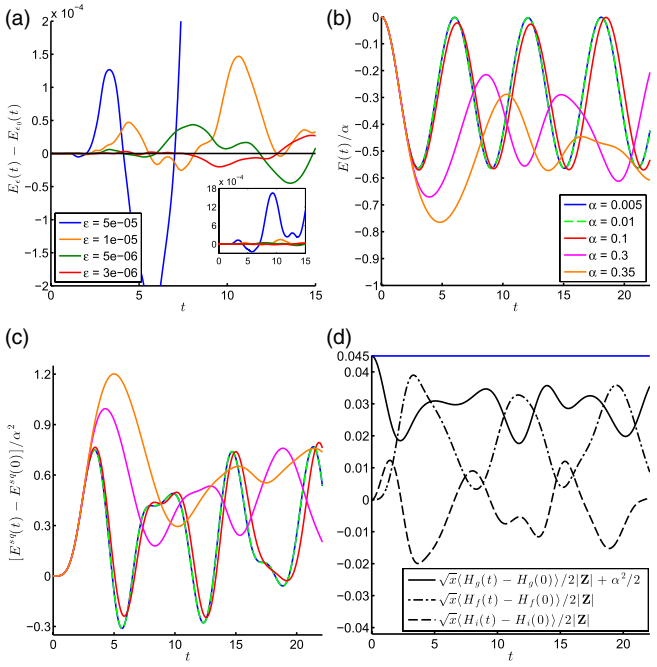

FIG. 2 (color online). Results for $m/g = 0.25$, $x = 100$, all quantities are in units $g = 1$. (a) Difference of $E(t) \equiv \langle\Psi_0(t)|L(1) + L(2)|\Psi_0(t)\rangle/2$ for various tolerances ϵ with respect to the estimated value for $\epsilon = \epsilon_0 = 2 \times 10^{-6}$ ($\alpha = 0.3$). (b) $E(t)/\alpha$ for different values of α. (c) $E^{sq}(t)/\alpha^2$, with $E^{sq}(t) \equiv \langle\Psi_0(t)|L^2(1) + L^2(2)|\Psi_0(t)\rangle/2$, for the same set of α values as in (b). (d): For $\alpha = 0.3$, the different energy densities of, respectively, the first (H_g), second (H_f), and third term (H_i) of Eq. (2) but with $L(n) \to L(n) + \alpha$ (we subtracted the values at $t = 0$ without background field). The straight blue line is the total energy density obtained as the sum of the three terms.

In Fig. 2(b) we display our result for the evolution of the electric field expectation value (minus the background value) for different values of α. For early times we clearly find the α-scaling behavior as predicted from linear response theory (see S5 of the Supplemental Material [14]). The $\alpha = 0.005$ and $\alpha = 0.01$ cases remain in the linear response regime throughout the entire depicted evolution; the periodic oscillations in this case can be traced back to the dominant production of the single-particle vector excitation in the linear response regime (see S5 of the Supplemental Material [14]). Larger values of α progressively depart from linear response, showing more complex behavior at later times. The physical picture here [21], which we study in more detail in Ref. [25], is that the charged fermionic particles that are created by a strong initial electric field in turn backreact onto this field.

In Fig. 2(c) we display the analogous result for the electric field squared expectation value. As the operator $\sum_n L^2(n)$ is now invariant under CT, this should scale as α^2 for early times (see S5 of the Supplemental Material [14]), which is indeed what we find. Finally, in Fig. 2(d) we show the evolution of the energies in the different sectors. We see that the energy which is initially injected in the first gauge

field term in (2) partially leaks into the second fermionic mass term and third kinetic or interaction term, as we can again qualitatively understand from the fermionic particle creation picture. In Ref. [22] a similar behavior was observed in the semiclassical limit. A last cross-check of our real-time results is then provided by the total energy conservation which is indeed satisfied, as can be seen from the blue line in Fig. 2(d).

Conclusions.—In this Letter we have demonstrated the potential of MPS as a numerical method for gauge theories. It is clear that we have only scratched the surface of this approach and that even within the Schwinger model there are many other types of calculations one could do, like, for instance, the construction of two-particle scattering states [28]. Looking further afield, one can easily generalize our gauge invariant MPS ansatz to other gauge groups like $SU(N)$ and also to higher dimensions. Explicitly for $d = 2 + 1$, the gauge-invariant $2d$ projected entangled pair states (PEPS) [8] construction now involves five-leg tensors with four virtual indices and one physical index (c is charge) on the sites, of the form $[B^c]_{(q_l,\alpha_{q_l}),(q_r,\alpha_{q_r}),(q_d,\alpha_{q_d}),(q_u,\alpha_{q_u})} = [b^c_{q_l,q_r,q_u}]_{\alpha_{q_l},\alpha_{q_r},\alpha_{q_d},\alpha_{q_u}} \delta_{q_l+q_d+c,q_r+q_u}$, while on the links we get a three-leg tensor with two virtual indices and one physical index (p is the electric field unit) $[C^p]_{(q_l,\alpha_{q_l}),(q,\alpha_{q_r})} = [c^p]_{\alpha_{q_l},\alpha_{q_r}} \delta_{q_l,p} \delta_{q_r,p}$.

We thank Mari-Carmen Bañuls for suggesting to us to look at real-time quench dynamics. Furthermore, we acknowledge very interesting discussions with Mari-Carmen Bañuls, David Dudal, and Lucca Tagliacozzo. This work is supported by an Odysseus grant from the FWO, a Ph.D. grant from the FWO (B. B), the FWF grants FoQuS and Vicom, the ERC grant QUERG, and the EU grant SIQS.

Note added.—Recently, Ref. [29] appeared with an approach that is conceptually close to ours. In that Letter, the authors use a quantum link model to write down gauge-invariant MPS for the Schwinger model.

[1] S. Dürr *et al.*, Science **322**, 1224 (2008); Z. Fodor and C. Hoelbling, Rev. Mod. Phys. **84**, 449 (2012).
[2] T. M. R. Byrnes, P. Sriganesh, R. J. Bursill, and C. J. Hamer, Nucl. Phys. B, Proc. Suppl. **109**, 202 (2002); T. M. Byrnes, P. Sriganesh, R. J. Bursill, and C. J. Hamer, Phys. Rev. D **66**, 013002 (2002); T. M. R. Byrnes, Ph.D. thesis, The University of New South Wales, 2003, http://books.google.co.jp/books?id=FwaiXgJWM2MC.
[3] M. C. Bañuls, K. Cichy, K. Jansen, and J. I. Cirac, J. High Energy Phys. 11 (2013) 158; M. C. Bañuls, K. Cichy, J. I. Cirac, K. Jansen, and H. Saito, *Proc. Sci.*, LAT2013 (2013) 332 [arXiv:1310.4118].
[4] T. Sugihara, J. High Energy Phys. 7 (2005) 022.
[5] L. Tagliacozzo and G. Vidal, Phys. Rev. B **83**, 115127 (2011).
[6] J. I. Cirac and F. Verstraete, J. Phys. A **42**, 504004 (2009).
[7] S. R. White, Phys. Rev. Lett. **69**, 2863 (1992).
[8] F. Verstraete and J. I. Cirac, arXiv:cond-mat/0407066.
[9] S. Elitzur, Phys. Rev. D **12**, 3978 (1975).
[10] E. Zohar, J. I. Cirac, and B. Reznik, Phys. Rev. A **88**, 023617 (2013).
[11] S. Coleman, Ann. Phys. (N.Y.) **101**, 239 (1976).
[12] C. Adam, Phys. Lett. B **382**, 383 (1996).
[13] J. Kogut and L. Susskind, Phys. Rev. D **11**, 395 (1975).
[14] See the Supplemental Material at http://link.aps.org/supplemental/10.1103/PhysRevLett.113.091601 for (S1) a proof of the general gauge invariant MPS form in Eq. (5), (S2) details on the TDVP method and one-particle excitations for gauge invariant MPS (in the presence of the *CT* symmetry), (S3) more details on the results for the ground state and excitations, (S4) details on the application of the iTEBD method for the real-time evolution of gauge invariant MPS, and (S5) the explicit derivation of the relevant expressions in the linear response regime.
[15] M. Fannes, B. Nachtergaele, and R. F. Werner, Commun. Math. Phys. **144**, 443 (1992).
[16] J. Haegeman, J. I. Cirac, T. J. Osborne, I. Pizorn, H. Verschelde, and F. Verstraete, Phys. Rev. Lett. **107**, 070601 (2011).
[17] J. Haegeman, B. Pirvu, D. J. Weir, J. I. Cirac, T. J. Osborne, H. Verschelde, and F. Verstraete, Phys. Rev. B **85**, 100408 (2012).
[18] J. Haegeman, T. J. Osborne, and F. Verstraete, Phys. Rev. B **88**, 075133 (2013).
[19] J. Schwinger, Phys. Rev. **82**, 664 (1951).
[20] S. Schmidt, D. Blaschke, G. Röpke, S. A. Smolyansky, A. V. Prozorkevich, and V. D. Toneev, Int. J. Mod. Phys. E **07**, 709 (1998).
[21] Y. Kluger, J. M. Eisenberg, B. Svetitsky, F. Cooper, and E. Mottola, Phys. Rev. D **45**, 4659 (1992).
[22] F. Hebenstreit, J. Berges, and D. Gelfand, Phys. Rev. D **87**, 105006 (2013).
[23] F. Gelis and N. Tanji, Phys. Rev. D **87**, 125035 (2013).
[24] D. Kawai, Y. Sato, and K. Yoshida, Phys. Rev. D **89**, 101901 (2014).
[25] B. Buyens, J. Haegeman, F. Verstraete, and K. Van Acoleyen (to be published).
[26] G. Vidal, Phys. Rev. Lett. **98**, 070201 (2007); R. Orús and G. Vidal, Phys. Rev. B **78**, 155117 (2008).
[27] M. Suzuki, Phys. Lett. A **146**, 319 (1990); N. Hatano and M. Suzuki, Lect. Notes Phys. **679**, 37 (2005).
[28] L. Vanderstraeten, J. Haegeman, T. J. Osborne, and F. Verstraete, Phys. Rev. Lett. **112**, 257202 (2014).
[29] E. Rico, T. Pichler, M. Dalmonte, P. Zoller, and S. Montangero, Phys. Rev. Lett. **112**, 201601 (2014).